Int J Clin Exp Pathol 2017;10(3):2917-2927
www.ijcep.com /ISSN:1936-2625/IJCEP0046596

Original Article

MiR-150 inhibits hypoxia-induced autophagy in oral squamous carcinoma by negatively regulating BNIP3

Yan-Jun Cui[1], Chao Liu[2], Fa-Wei Pang[1], Guang-Ping Liu[1], Jian-Hua Zhou[1], Xiao-Ming Shi[2], Sheng-Yun Huang[2], Dong-Sheng Zhang[1,2]

[1]Department of Oral and Maxillofacial Surgery, School of Stomatology, Shandong University, Jinan, China; [2]Department of Oral and Maxillofacial Surgery, Shandong Provincial Hospital Affiliated to Shandong University, Jinan, Shandong, China

Received December 14, 2016; Accepted December 27, 2016; Epub March 1, 2017; Published March 15, 2017

Abstract: Oral squamous cell carcinoma (OSCC) is a malignant solid tumor characterized by hypoxia. Autophagy is considered to play a protective role in cancer cells under hypoxia. A variety of microRNAs (miRNAs) that play a critical role in tumorigenesis have been identified. However, the underlying mechanisms of miR-150 in OSCC development remain unclear. In this study, we observed decreased downregulated expression of miR-150 in association with increased expression of BNIP3 in CAL-27 cells under hypoxia. Hypoxia induced the initiation of the BNIP3-mediated autophagic process, and overexpression of miR-150 inhibited hypoxia-induced autophagy. In addition, we demonstrated that miR-150 inhibited autophagy by negatively regulating the expression of the BNIP3 gene. Collectively, our study identified miR-150 as a key modulator of autophagy by inhibiting BNIP3 in OSCC cells.

Keywords: miR-150, autophagy, oral squamous carcinoma, BNIP3

Introduction

Oral squamous cell carcinoma (OSCC) is the most common type of cancer in the oral cavity, with an estimated global incidence of more than 500,000 annually, including 300,000 newly diagnosed cases and an annual mortality of approximately 145,000 [1, 2]. Because most OSCCs are diagnosed in the advanced stage, patients frequently develop a second primary cancer, local recurrence, and distant metastasis after treatment failure [3]. At present, the treatment modalities for OSCC involve radical surgical resection with adjuvant chemotherapy, radiotherapy, or both. In spite of great improvements in the prevention of oral cancer, little improvement in the relative 5-year survival rate of patients with OSCC has been observed in the past several decades [4]. Hence, the understanding of the molecular mechanisms related to the pathogenesis and progression of this disease could allow to establish new and more effective therapeutic strategies to improve the survival and quality of life of patients.

Autophagy is a lysosomal degradation pathway whereby degrades long-lived cellular macromolecules and organelles [5, 6], and maintains intracellular homeostasis and prolongs cell survival under stress. Autophagy is up-regulated in response to stress conditions such as nutrient deprivation, growth factor depletion, and hypoxia [7-9]. Emerging evidence suggested that the autophagy is related to a variety of pathological disorders including cancer, neurodegenerative and cardiovascular diseases [10-12]. In cancer cells, autophagy appears to play a role at multiple levels of tumor development and may have a protective role in carcinogenesis [13], and the elucidation of the exact role of autophagy at different stages of cancer progression and in treatment responsiveness is a complex and challenging task. Further uncovering the role of autophagy in OSCC might lead to the identification of novel strategies for OSCC treatment.

Recently, a novel class of endogenous small non-coding gene regulatory RNAs, termed microRNA (miRNAs), has gained significant attention [14]. MiRNAs exert their regulatory functions on the expression of multiple genes by initiating translational silencing or degradation of their cognate target mRNA [15, 16].

Accumulating evidence shows that miRNAs play important roles in the regulation of most cellular processes, including differentiation, proliferation, apoptosis, metabolism and autophagy [17-20]. Deregulation of miRNAs is closely linked to the pathological mechanisms of many human diseases, including cancer [21]. Several studies have also shown that miR-150 is frequently downregulated in pancreatic cancer, esophageal cancer, colorectal cancer, and liver cancer [22-25], suggesting a tumor-suppressive role of miR-150 in human tumorigenesis. However, the biological functions and mechanisms of miRNA-150 in OSCC are unclear.

Materials and methods

Reagents and antibodies

Human miR-150 mimic and mimic negative controls (miR-NC) were purchased from Ribobio (Guangzhou, China). MiR-150 inhibitor and inhibitor negative control (miR-NC) were also purchased from Ribobio (Guangzhou, China). Transfection of miRNA was performed with a riboFECTTM Transfection Kit (Ribobio, Guangzhou, China) according to the manufacturer's protocol. The following primary antibodies were used for Western blot: anti-BNIP3 polyclonal antibody, anti-HIF-1 polyclonal antibody, anti-LC3B polyclonal antibody, anti-Beclin1 monoclonal antibody, anti-Atg5 monoclonal antibody, anti-p62 monoclonal antibody, and anti-actin polyclonal antibody (Abcam, Cambridge, MA, USA). Fluorescein isothiocyanate-labeled goat anti-rabbit IgG antibody Invitrogen (Thermo Fisher Scientific, Inc., Waltham, MA, USA) was used as a fluorescent secondary antibody. Alexa Fluor 488-labeled goat anti-rabbit IgG antibody (Beijing ComWin Biotech Co., Ltd., Beijing, China) was used as the secondary antibody for western blot.

Cell culture and transfection

The OSCC cell line CAL-27 was obtained from Ninth People's Hospital, Shanghai Second Medical University. All cells were cultured in Dulbecco's modified eagle medium (DMEM) (Invitrogen, Carlsbad, CA, USA) supplemented with 10% fetal bovine serum (Thermo Fisher, Waltham, MA, USA), 100 μM penicillin, and 100 μM streptomycin (Invitrogen, Carlsbad, CA, USA) in a humidified 5% CO_2 environment at 37°C. Hypoxic conditions were achieved with a gas-controlled chamber (Thermo Electron Corp., Marietta, OH, USA) maintained at 1% O_2, 94% N_2, and 5% CO_2 at 37°C. A total of 1×10^5 CAL-27 cells were seeded on six-well plates, and after reaching 60-70% confluence, the cells were transfected with miR-150 mimic (and mimic negative control) or inhibitor (and inhibitor negative control) at concentrations ranging from 50 to 100 nM using a riboFECTTM Transfection Kit (Ribobio, Guangzhou, China) according to the manufacturer's instructions. The cells were washed 16 h after transfection, replenished with complete medium, and harvested at 24 or 48 h after transfection for subsequent analysis. Quantitative real-time polymerase chain reaction (qRT-PCR) was used to verify the efficiency of transfection.

RNA extraction and qRT-PCR

Total RNA was extracted from harvested cells using TRIzol reagent (Takara Biotechnology, Co., Ltd., Dalian, China) according to the manufacturer's instructions. The concentration and purity of RNA were determined spectrophotometrically using a NanoDrop ND-1000 (NanoDrop Technologies, Wilmington, DE, USA). The ratio of A260:A280 was used to indicate the purity of the total RNA. A two-step qRT-PCR was performed using a PrimeScript™ RT reagent kit (Takara Biotechnology, Co., Ltd., Dalian, China). The total RNA was converted into cDNA using a PrimeScript™ RT reagent kit (Takara Biotechnology, Co., Ltd., Dalian, China). Then, significantly up-regulated or down-regulated miRNAs were quantified by real-time PCR using SYBRRPremix Ex Taq TM (Takara Biotechnology, Co., Ltd., Dalian, China). PCR was performed in a real-time PCR system (Roche Light Cycler 480 Germany) as follows: 95°C for 3 min, 35 cycles of 95°C for 5 sec, 60°C for 20 sec and 72°C for 30 sec, and then 94°C for 1 min and 60°C for 1 min, with the addition of a cycle for every 0.5°C. The relative expression levels of BNIP3 and miR-150 were respectively normalized to GAPDH and U6. The following gene-specific primers were used: Three independent experiments were performed in triplicate.

Western blot analysis

Protein extraction and western blot were performed as described previously [26, 27]. Cells

were washed twice with cold phosphate-buffered saline (PBS) and lysed on ice in RIPA buffer (Shennong Bocai Biotechnology Co., Ltd., Shanghai, China). After incubation on ice for 30 min, the lysates were cleared by centrifugation at 14,000 g for 15 min at 4°C, and the protein concentrations were determined using BCA protein assay kits (Shennong Bocai Biotechnology Co., Ltd., Shanghai, China). Equal amounts of total protein were loaded and separated by 10-15% sodium dodecyl sulfate-polyacrylamide gel electrophoresis (Shennong Bocai Biotechnology Co., Ltd., Shanghai, China) and transferred to PVDF membranes (Shennong Bocai Biotechnology Co., Ltd., Shanghai, China). After blocking with 5% nonfat milk in phosphate-buffered saline, the membranes were incubated with specific primary antibodies overnight at 4°C, followed by incubation with secondary antibodies labeled with HRP for 60 min. After washing three times with TBST, the proteins were visualized using an Alpha Imager 2200 system (Alpha Innotech Corporation, San Leandro, CA, USA). The bands of the specific proteins were quantified after normalization to the density of actin using Image J instrument software.

Immunofluorescence microscopy

A total of 2×10^5 CAL-27 cells were seeded in 12-well plates with 14-mm-diameter coverslips. After incubation for at least 24 h, the cells were treated with miR-150 mimic (and mimic negative control), miR-150 inhibitor (and inhibitor negative control) for 48 h under hypoxia (1% O_2) or normoxia (20% O_2). The cells were then fixed in 4% paraformaldehyde (Beijing ComWin Biotech Co., Ltd., Beijing, China) for 20 min and permeabilized in 0.2% Triton X-100 (Beijing ComWin Biotech Co., Ltd., Beijing, China) for 10 min. After washing three times with PBS, the slices were blocked with goat serum for 1 h at room temperature (RT), then incubated with rabbit polyclonal anti-BNIP3 antibody (1:100 diluted in PBS) at 4°C overnight. The next day, the cells were washed three times with PBS and incubated for 1 h with goat anti-rabbit immunoglobulin (Ig) antibody conjugated with fluorescein isothiocyanate (FITC; Beijing ComWin Biotech Co., Ltd., Beijing, China) (1:400 diluted in PBS) for 1 h at room temperature in the dark. Nuclei were counterstained with DAPI (BeijingComWin Biotech Co., Ltd., Beijing, China). After washing with PBS, cells were mounted with antifade mounting media (BeijingComWin Biotech Co., Ltd., Beijing, China), and signals were visualized under a Nikon-E600 fluorescence microscope (TE2000; Nikon Corporation, Tokyo, Japan). Images were recorded using RSImage software.

Transmission electron microscopy

The CAL-27 cells (1×10^6) were seeded in 6-well plates. After reaching 70-80% confluence, the cells were transfected with miR-150 mimic (and mimic negative control), miR-150 inhibitor (and inhibitor negative control) using the riboFECTTM Transfection Kit (Ribobio, Guangzhou, China) according to the manufacturer's protocol, followed by culture for 48 h under hypoxia (1% O_2) or normoxia (20% O_2). The cells were then fixed with 2% glutaraldehyde in 0.1 M Sorensen buffer (pH 7.3; Beijing Chemical Industry Group, Co., Ltd., Beijing, China) for 1 h at 4°C and post-fixed in 1% osmium tetroxide in 0.1 M cacodylate buffer for 1 h at room temperature. The cells were then dehydrated in solutions of ethanol (30-90%), embedded in epon resin (Beijing Chemical Industry Group, Co., Ltd., Beijing, China) and sliced with a UC7 microtome (Leica, Wetzlar, Germany) to a 70-nm thickness and placed on uncoated copper grids. Sections were subsequently counterstained with 4% uranyl acetate (Beijing Chemical Industry Group, Co., Ltd., Beijing, China) and visualized using a JEM-1200EX Transmission Electron Microscope (JEOL, Ltd., Tokyo, Japan).

Statistical analysis

Differences between groups were analyzed using a Student's t-test. All data were presented as the mean ± standard deviation from the three independent experiments and analyzed using SPSS software, version 19.0 (IBM SPSS, Armonk, NY, USA). $P<0.05$ was considered as statistically significant difference.

Results

Expression level of miR-150 and BNIP3 in hypoxia-induced CAL-27 cells

To determine the expression levels of miR-150 and BNIP3 in CAL-27 cells, we first measured the expression of mature miR-150 and BNIP3 in CAL-27 cells under hypoxia (1% O_2) and nor-

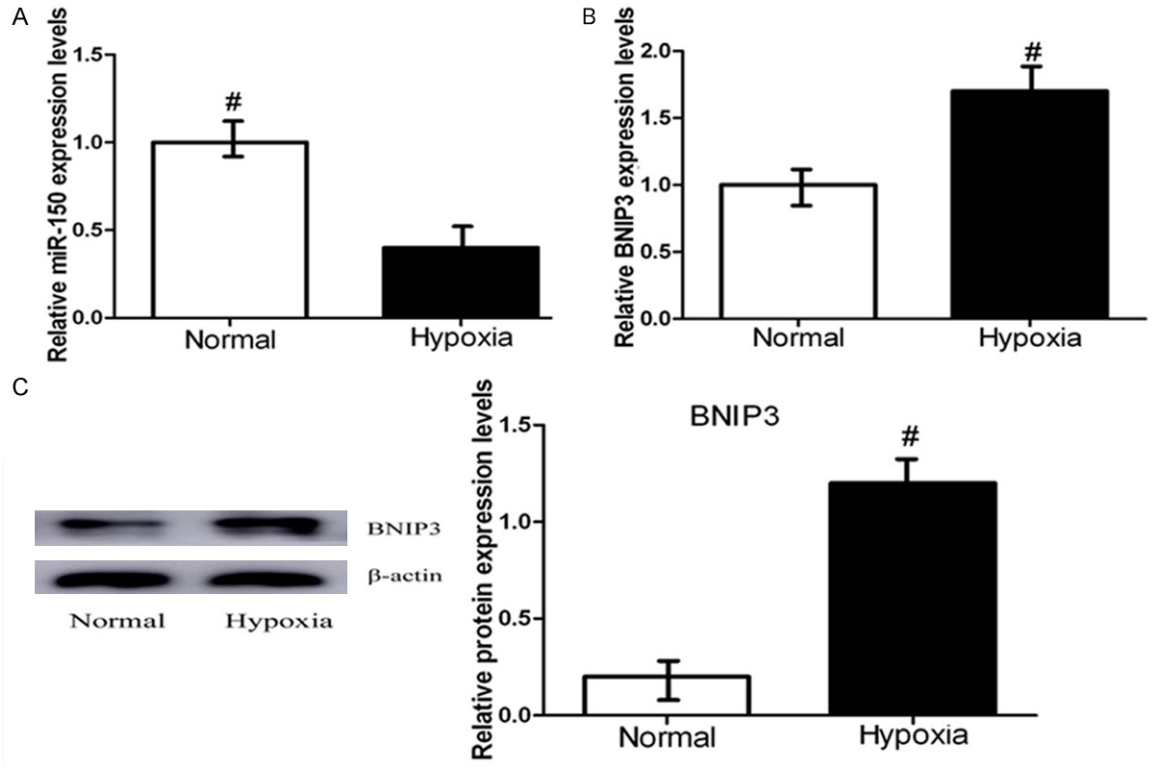

Figure 1. Expression levels of miR-150 and BNIP3 in hypoxia-induced CAL-27 cells. CAL-27 cells were cultured under normoxia or hypoxia for 24 h. A, B. The relative mRNA expression levels of miR-150 and BNIP3 under hypoxia and normoxia were detected by qRT-PCR. U6 was used as an internal control. #P<0.05. C. Western blot analysis of the protein expression of BNIP3 between hypoxia and normoxia. β-actin was used as an internal control. #P<0.05. All data are the mean ± SD of three independent experiments.

moxia (20% O_2) by qRT-PCR. As shown in **Figure 1A**, miR-150 levels were decreased significantly following culture in hypoxic conditions compared with normal cell lines. **Figure 1B** shows that the expression of BNIP3 in OSCC CAL-27 cells was significantly increased under hypoxia compared with normoxia. We further examined the protein level of BNIP3 in CAL-27 cells by Western blot, which revealed that the BNIP3 protein level was higher in CAL-27 cells than in normal cell lines (**Figure 1C**). These results demonstrate that hypoxia may decrease the expression of miRNA-150 and increase the expression of BNIP3.

Hypoxia induces autophagy in CAL-27 cells

One of the physiological responses of hypoxia is the induction of autophagy [28]. To investigate whether autophagy could be induced by hypoxia in OSCC cell lines, CAL-27 cells were incubated under hypoxic conditions for 4, 8, 16, and 24 h. When autophagy is activated, the LC3-I protein localized in the cytoplasm is cleaved, lipidated, and inserted as LC3-II into autophagosome membranes [29], providing a means of observing autophagy induction. As shown in **Figure 2A**, a diffuse distribution of green fluorescence and weak punctate dots were observed under normoxia, whereas a cornucopia of LC3 punctate dots in the cytoplasm was observed under hypoxic conditions by fluorescence microscopy. Transmission electron microscopy analysis revealed an increase in double-membrane-bound vacuoles, where cytoplasmic material and/or membrane vesicles were encapsulated in vacuoles, the gold standard for determination of autophagy in CAL-27 cells incubated at 1% O_2 compared with 20% O_2 (**Figure 2B**, black arrows). During autophagy, a series of autophagy genes associated with the formation of autophagosomes are highly activated [30]. To confirm hypoxia-induced autophagy, western blot analyses were performed to measure the expression of LC3, Atg5, Beclin1 and P62 at the protein levels. We

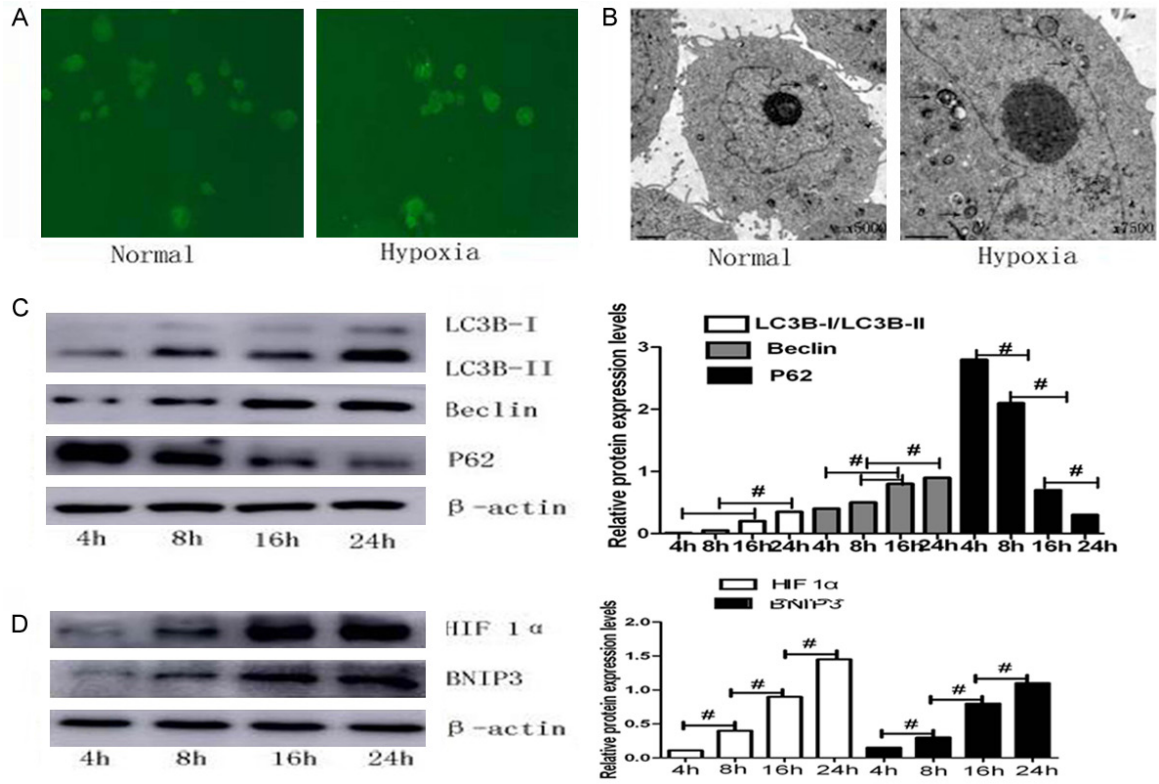

Figure 2. Hypoxia induces autophagy in CAL-27 cells. CAL-27 cells were cultured under normoxia or hypoxia for 4, 8, 16, and 24 h. A. LC3 punctate dots were visualized by fluorescence microscopy after CAL-27 cells were incubated under normoxic or hypoxic conditions for 24 h. Nuclei were stained with DAPI. The LC3 punctate dots were quantified by randomly counting 10 cells for each group. B. Autophagosomes or lysosomes containing segregated and degraded organelles, cytoplasmic material and/or membrane vesicles were observed by transmission electron microscopy after exposure to normoxic or hypoxic conditions for 24 h. Black arrows indicate autophagic vacuoles consisting of double membranes. (× 10000 magnification). The number of double membrane vacuoles per cell was determined by counting 20 cells for each sample. C. Time-dependent expression of autophagy-related genes following hypoxic exposure was assayed by western blot. β-actin was used as the internal control. #P<0.05. D. The time-dependent expression of hypoxia-induced protein HIF-1α/BNIP3 following hypoxic exposure was assayed by western blot. β-actin was used as the internal control. #P<0.05. All data are the mean ± SD of three independent experiments.

observed that hypoxia increased the expression of LC3, Atg5, and Beclin1 in a time-dependent manner (**Figure 2C**). As HIF-1 is the key protein responsible for cellular adaptation to low oxygen conditions, we examined whether HIF-1 was involved in the hypoxia-induced autophagy. Our results also showed that cells subjected to hypoxia presented increased protein levels of HIF-1 and BNIP3 in hypoxia-treated CAL-27 cells (**Figure 2D**). These results suggest that hypoxia could induce the presence of the double membrane of autophagic vesicles and expression of autophagy-related proteins, including BNIP3, after 24 h of hypoxia. Taken together, these results demonstrate that autophagy might be induced during oxygen hypoxic stress and that initiation of the autophagic process is mediated through HIF-1 signaling in CAL-27 cells.

miR-150 inhibits hypoxia-induced autophagy in CAL-27 cells

Emerging evidence indicates that miRNA regulates autophagy by targeting autophagy-related genes [31-33]. To investigate if miR-150 modulates autophagy under hypoxia, we transfected CAL-27 cells with miR-150 mimic or negative control (miR-NC) under hypoxia for 48 h. Our data showed that the number of LC3 punctate dots formed per cell significantly decreased in cells transfected with miR-150 mimic (**Figure 3A**). In addition, the number of autophagolysosomes was lower after miR-150 treatment than miR-NC treatment, as observed by transmission electron microscopy (**Figure 3B**). The inhibitory effects of miR-150 on autophagy were also confirmed by western blot analysis. Consistent with the other markers of autopha-

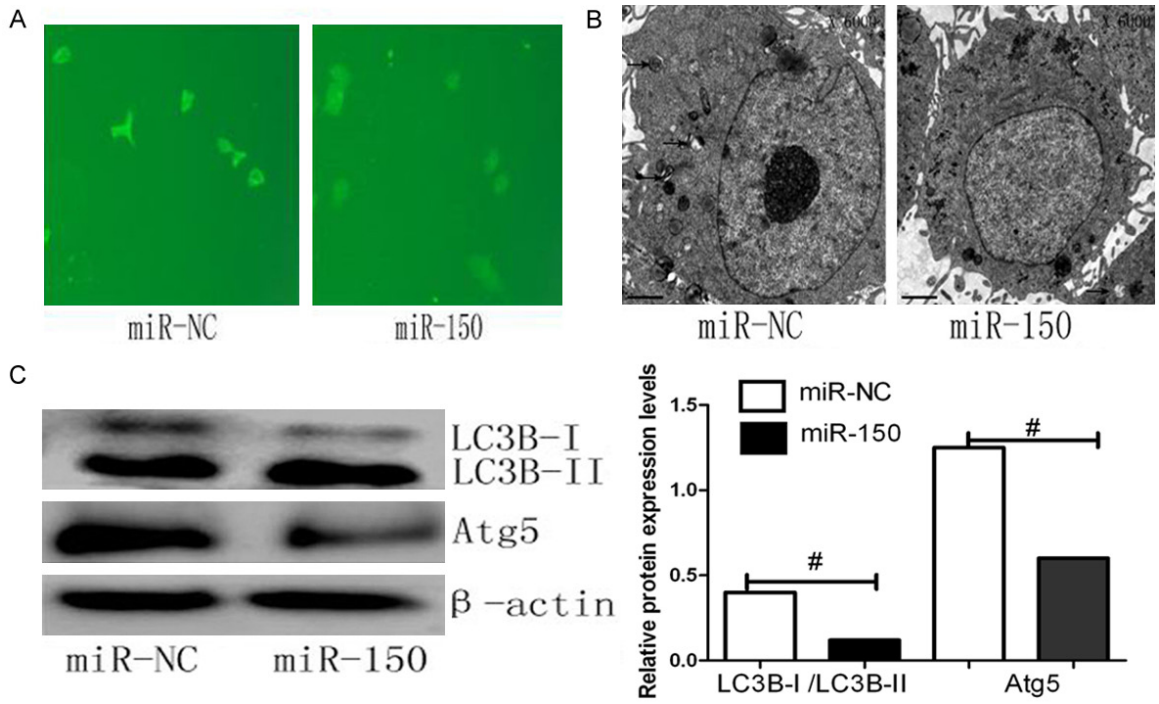

Figure 3. miR-150 inhibits hypoxia-induced autophagy in CAL-27 cells. CAL-27 cells were transfected with miR-150 mimic or negative control (50 nM) under a hypoxic environment for 24 h. A. LC3 punctate dots were visualized by fluorescence microscopy. The LC3 puncta were quantified by randomly counting 10 cells for each group. B. Autophagosomes or lysosomes containing segregated and degraded organelles were observed by transmission electron microscopy. Black arrows indicate autophagic vacuoles consisting of double membranes. (× 6000 magnification). The number of double membrane vacuoles per cell was determined by counting 20 cells for each sample. C. The relative protein expression levels of LC3B-I to LC3B-II conversion and Atg5 were assayed by western blot. β-actin was used as an internal control. #P<0.05. All data are the mean ± SD of three independent experiments.

gy inhibition, we observed that following treatment with miR-150 mimic, the LC3B-II/LC3B-I ratio was attenuated, and polyubiquitin-binding protein p62 levels were increased after overexpression of miR-150 (**Figure 3C**). These results indicated that endogenous miR-150 contributes to the limitation of autophagic responses in CAL-27 cells and that miR-150 may be a novel inhibitor of autophagy.

miR-150 negatively regulates the BNIP3 protein in CAL-27 cells under hypoxia

Because precise modulation of BNIP3 protein levels is essential for tumorigenesis, we hypothesized that BNIP3 is regulated through a miR-mediated mechanism. Since bioinformatics analysis indicated that miR-150 is inversely correlated correlation with BNIP3 in OSCC, we next verified whether miR-150 can regulate endogenous BNIP3 expression under hypoxia. CAL-27 cells were transiently transfected with miR-150 mimic or inhibitor, and the expression of BNIP3 was examined. **Figure 4A**, **4B** validation miR-150 after transfected with miR-150 mimic or inhibitor. Western blot analysis revealed that the protein expression levels of BNIP3 were clearly decreased by the miR-150 mimic compared with the negative control after 48 h (**Figure 4C**). By contrast, BNIP3 protein levels were significantly increased in miR-150 inhibitor-transfected cells compared with negative control-transfected cells under hypoxia (**Figure 4D**). Taken together, we can conclude that miR-150 negatively regulates the protein expression of BNIP3 in CAL-27 cells under hypoxia.

Discussion

A variety of miRNAs have been identified to play a critical role in tumorigenesis, and important regulatory functions of miRNAs in several biological processes associated with tumor have been described [34]. However, the underlying mechanisms of miRNAs in OSCC development have not been fully elucidated. To understand the impact and molecular mechanisms underlying miRNA function, we searched for target

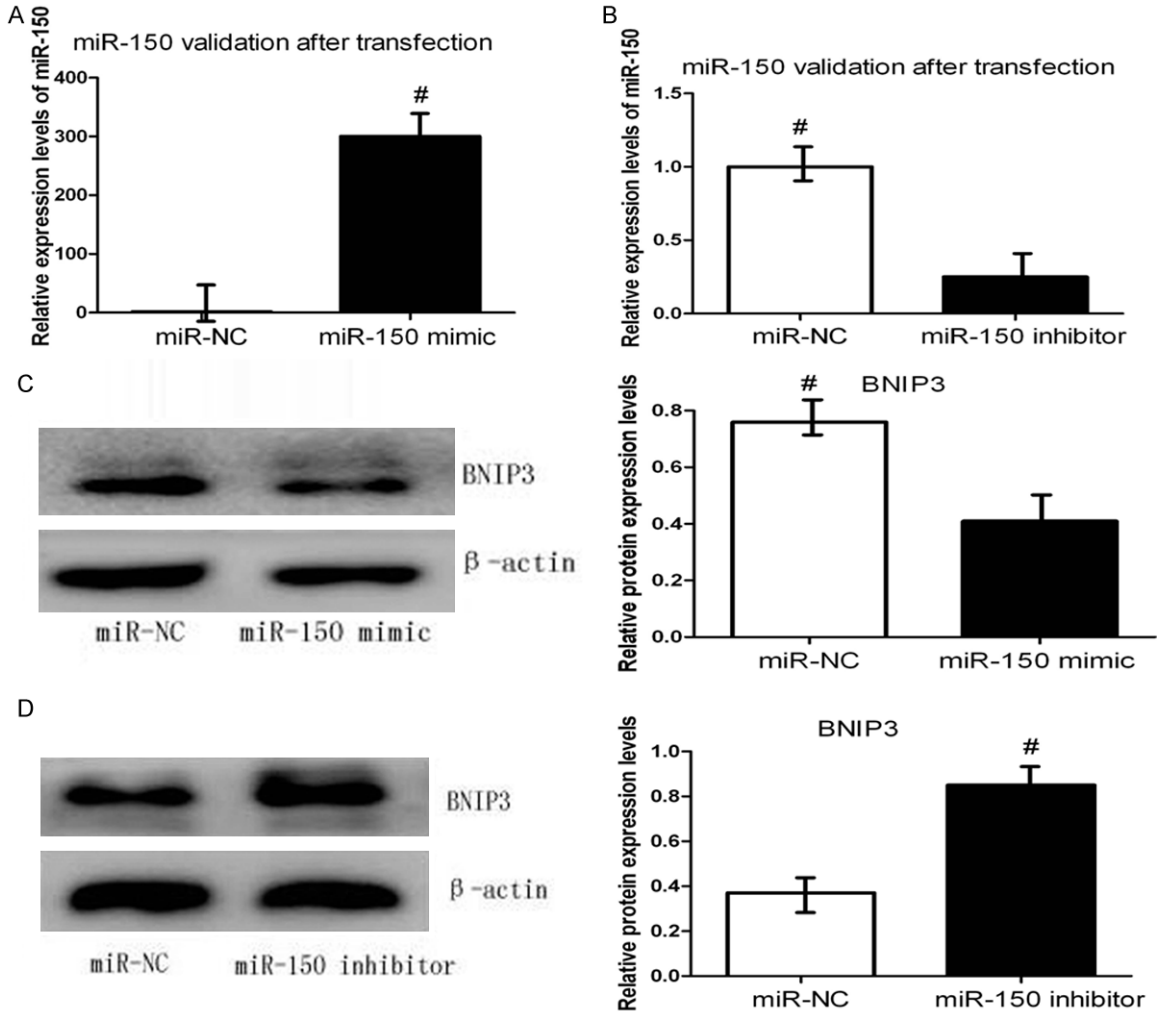

Figure 4. miR-150 negatively regulates BNIP3 protein levels in CAL-27 cells under hypoxia. A and B. Validation miR-150 after transfected with miR-150 mimic or inhibitor. C. The protein expression of BNIP3 in CAL-27 cells was detected by western blot after transfection with miR-150 mimic (50 nM) or negative control (50 nM) under hypoxia (48 h). D. The protein expression of BNIP3 in CAL-27 cells was detected by western blot after transfection with miR-150 inhibitor (100 nM) or negative control (100 nM) under hypoxia (48 h). β-actin was used as the internal control. #P<0.05. All data are the mean ± SD of three independent experiments.

genes that might be regulated by miR-150. We demonstrated here that hypoxia resulted in decreased expression of miR-150 in CAL-27 cells in association with increased expression of BNIP3. Forced overexpression of miR-150 inhibited autophagy of CAL-27 cells. Additionally, the upregulation of miR-150 negatively regulated the protein levels of BNIP3. These results suggest that miR-150 is a key modulator of autophagy by inhibiting BNIP3 in OSCC cells.

MiRNAs play vital roles by regulating the expression of target genes via the degradation or translational inhibition of their target mRNAs [35-37]. A growing body of evidence now suggests that miRNAs act either as oncogenes or tumor suppressors in a variety of cancers [38, 39]. To determine the role of miR-150 in OSCC, we searched for physiological targets using bioinformatics analysis. Bcl-2 nineteen-kilodalton interacting protein (BNIP3), a BH3-only member of the Bcl-2 family, was identified as one of the targets of miR-150. BNIP3 is increased in many cancers, such as gastric adenocarcinomas, breast cancer, non-small cell lung cancer, and primary prostate tumors [40-43]. During the past decades, a series of studies have suggested that increased expression of BNIP3 might induce cell death through multiple pathways including apoptosis, necrosis and autophagy, depending on cell lines and conditions [44-46]. Recent work provides further evidence

that overexpression of BNIP3 is not sufficient to induce cell death and defines a role for BNIP3 in promoting autophagy in response to hypoxia [47]. BNIP3 competes with Beclin1-Bcl2 and Beclin1-Bcl-xl complexes, resulting in release of Beclin1 and thus enhancing autophagy [48, 49]. BNIP3 induces autophagy by interacting with RheB, resulting in mTOR inhibition [50]. Moreover, BNIP3 could be involved in autophagosome-lysosome fusion in later stages of autophagy [51, 52]. Here, we found that the expression of BNIP3 was significantly increased in CAL-27 cells under hypoxia exposure compared to normoxia. Transfection of miR-150 mimic decreased the protein levels of BNIP3 in CAL-27 cells under hypoxia exposure, whereas administration of the miR-150 inhibitor increased BNIP3 protein levels compared with the negative control. These results suggest that BNIP3 protein levels are inversely associated with miR-150 expression in CAL-27 cells, which suggest that miR-150 might be an important factor in OSCC cells through directly targeting BNIP3. Further studies exploring the role BNIP3 as a novel target in therapeutic applications are needed.

Recently, the role of miRNAs in tumorigenesis has been widely investigated, and their important regulatory functions in several biological processes associated with tumors have been described [34]. Among known miRNAs with significantly decreased expression levels, the highly conserved miRNA miR-150 attracted our attention. Decreased levels of miR-150 have been observed in esophageal carcinoma, colorectal cancer, pancreatic cancer, chronic lymphocytic leukemia, and liver cancer [23-25, 53, 54], whereas miR-150 is upregulated in gastric cancer, breast cancer, and lung cancer [55-57]. Aberrant expression of miR-150 is associated with cancer development and progression through regulating oncogenes or tumor suppressor genes [58-60]. Based on the literature, we explored the biological function of miR-150 expression in OSCC. Our results revealed decreased expression of miR-150 in CAL-27 cells under hypoxic conditions compared to normal conditions. Forced overexpression of miR-150 inhibited autophagy of CAL-27 cells. Our findings provide evidence suggesting that miR-150 plays an important role in modulating autophagosome formation in OSCC cells. Hence, identifying the specific involvement of miR-150 in oral squamous cell carcinogenesis will help expand our understanding of OSCC and aid the development of new targets for diagnosis and therapy.

In summary, our study suggests that miR-150 exerts its roles in OSCC through negative regulation of the protein levels of BNIP3, and overexpression of miR-150 inhibited autophagy in CAL-27 cells in vitro. These findings suggest that miR-150 may be a potential novel predictor and therapeutic target for future development of specific therapeutic interventions in OSCC. However, further studies with in vivo observations are required to confirm our results.

Acknowledgements

We thank all the staff members in laboratory center for the technical help and critical reading of the manuscript. This study was supported by grants from the National Natural Science Foundation of China (2016WS0410), and the Shandong Provincial Natural Science Foundation (grant no. ZR2016HQ041).

Disclosure of conflict of interest

None.

Address correspondence to: Dong-Sheng Zhang and Sheng-Yun Huang, Department of Oral and Maxillofacial Surgery, Shandong Provincial Hospital Affiliated to Shandong University, 324 Jingwu Road, Jinan 250021, Shandong, China. E-mail: ds63zhang@sdu.edu.cn (DSZ); huangsy28@163.com (SYH)

References

[1] Ferlay J, Soerjomataram I, Ervik M, Dikshit K, Eser S, Mathers C. GLOBOCAN 2012 v1.0, cancer incidence and mortality worldwide: IARC CancerBase No. 11. Lyon, France: International Agency for Research on Cancer; 2013.

[2] Rivera C. Essentials of oral cancer. Int J Clin Exp Pathol 2015; 9: 11884-94.

[3] Forastiere A, Koch W, Trotti A, Sidransky D. Head and neck cancer. N Engl J Med 2001; 26: 1890-900.

[4] Gupta S, Kong W, Peng Y, Miao Q, Mackillop WJ. Temporal trends in the incidence and survival of cancers of the upper aerodigestive tract in ontario and the United States. Int J Cancer 2009; 9: 2159-65.

[5] Klionsky DJ. Autophagy: from phenomenology to molecular understanding in less than a decade. Nat Rev Mol Cell Biol 2007; 11: 931-7.

[6] Yang Z, Klionsky DJ. Eaten alive: a history of macroautophagy. Nat Cell Biol 2010; 9: 814-22.
[7] Mihaylova MM, Shaw RJ. The AMPK signalling pathway coordinates cell growth: autophagy and metabolism. Nat Cell Biol 2011; 9: 1016-23.
[8] Levine B, Kroemer G. Autophagy in the pathogenesis of disease. Cell 2008; 1: 27-42.
[9] Zhang H, Bosch-Marce M, Shimoda LA, Tan YS, Baek JH, Wesley JB, Gonzalez FJ, Semenza GL. Mitochondrial autophagy is an HIF-1-dependent adaptive metabolic response to hypoxia. J Biol Chem 2008; 16: 10892-903.
[10] Lee JH, Yu WH, Kumar A, Lee S, Mohan PS, Peterhoff CM, Wolfe DM, Nixon RA. Lysosomal proteolysis and autophagy require presenilin 1 and are disrupted by Alzheimer-related PS1 mutations. Cell 2010; 7: 1146-58.
[11] Luo J, Solimini NL, Elledge SJ. Principles of cancer therapy: oncogene and non-oncogene addiction. Cell 2009; 5: 823-37.
[12] Garcia-Arencibia M, Hochfeld WE, Toh PP, Rubinsztein DC. Autophagy: a guardian against neurodegeneration. Semin Cell Dev Biol 2010; 7: 691-8.
[13] Fan TF, Bu LL, Wang WM. Tumor growth suppression by inhibiting both autophagy and STAT3 signaling in HNSCC. Oncotarget 2015; 41: 43581-93.
[14] Hardy BG, Schentag JJ. Lack of effect of cimetidine on the metabolism of quinidine: effect on renal clearance. Int J Clin Pharmacol Ther Toxicol 1988; 8: 388-91.
[15] Bartel DP. MicroRNAs: target recognition and regulatory functions. Cell 2009; 3: 215-33.
[16] Qin X, Xu H, Gong W, Deng W. The Tumor cytosol miRNAs, fluid miRNAs, and exosome miRNAs in lung cancer. Front Oncol 2014; 4: 357-65.
[17] Li YJ, Wang HX, Tao K, Xiao Q, Huang Z, Zhong L, Cao W, Wen J, Feng W. miR-29b suppresses CML cell proliferation and induces apoptosis via regulation of BCR/ABL1 protein. Exp Cell Res 2013; 8: 1094-01.
[18] He X.Q, Dong Y.J, Wu C.W , Zhao Z, Ng SS, Chan FK, Sung JJ, Yu J. MicroRNA-218 Inhibits Cell cycle progression and promotes apoptosis in colon cancer by downregulating BMI1 polycomb ring finger oncogene. Mol Med 2012; 12: 1491-98.
[19] Feng LF, Ma YN, Sun J, Shen Q, Liu L, Lu H, Wang F, Yue Y, Li J, Zhang S, Lin X, Chu J, Han W, Wang X, Jin H. YY1-MIR372-SQSTM1 regulatory axis in autophagy. Autophagy 2014; 8: 1442-53.
[20] Li Y, Chen D, Jin L, Liu J, Li Y, Su Z, Qi Z, Shi M, Jiang Z, Yang S, Lai Y. Oncogenic microRNA-142-3p is associated with cellular migration, proliferation and apoptosis in renal cell carcinoma. Oncol Lett 2016; 2: 1235-41.
[21] Sun LG, Liu L, Fu HH, Wang Q, Shi Y. association of decreased expression of serum mir-9 with poor prognosis of oral squamous cell carcinoma patients. Med Sci Monit 2016; 22: 289-94.
[22] Srivastava SK, Bhardwaj A, Singh S, Arora S, Wang B, Grizzle WE, Singh AP. MicroRNA-150 directly targets MUC4 and suppresses growth and malignant behavior of pancreatic cancer cells. Carcinogenesis 2011; 12: 1832-39.
[23] Yokobori T, Suzuki S, Tanaka N, Inose T, Sohda M, Sano A, Sakai M, Kuwano H. miR-150 is associated with poor prognosis in esophageal squamous cell carcinoma via targeting the EMT inducer ZEB1. Cancer Sci 2013; 1: 48-54,.
[24] Perilli L, Pizzini S, Bisognin A, Mandruzzato S, Biasiolo M, Facciolli A, Zanovello P. Human miRNome profiling in colorectal cancer and liver metastasis development. Genom Data 2014; 2: 184-98,.
[25] Zhang J, Luo N, Luo Y, Peng Z, Zhang T, Li S. microRNA-150 inhibits human CD133-positive liver cancer stem cells through negative regulation of the transcription factor c-Myb. Int J Oncol 2012; 3: 747-56.
[26] Singh S, Srivastava SK, Bhardwaj A, Owen LB, Singh AP. CXCL12-CXCR4 signalling axis confers gemcitabine resistance to pancreatic cancer cells: a novel target for therapy. Br J Cancer 2010; 11: 1671-79.
[27] Singh AP, Moniaux N, Chauhan SC, Meza JL, Batra SK. Inhibition of MUC4 expression suppresses pancreatic tumor cell growth and metastasis. Cancer Res 2004; 4: 622-30.
[28] Mazure NM, Pouyssegur J. Hypoxia-induced autophagy. cell death or cell survival? Curr Opin Cell Biol 2010; 2: 177-80.
[29] Tanida I, Ueno T, Kominami E. LC3 conjugation system in mammalian autophagy. Int J Biochem Cell Biol 2004; 12: 2503-18.
[30] Nakatogawa H, Suzuki K, Kamada Y, Ohsumi Y. Dynamics and diversity in autophagy mechanisms: lessons from yeast. Nat Rev Mol Cell Biol 2009; 7: 458-67.
[31] Chang Y, Yan W, He X, Zhang L, Li C, Huang H, Nace G, Geller DA, Lin J, Tsung A. miR-375 inhibits autophagy and reduces viability of hepatocellular carcinoma cells underhypoxic conditions. Gastroenterology 2012; 1: 177-87.e8.
[32] Frankel LB, Lund AH. MicroRNA regulation of autophagy. Carcinogenesis 2012; 11: 2018-25.
[33] Kovaleva V, Mora R, Park YJ, Plass C, Chiramel AI, Bartenschlager R, Döhner H, Stilgenbauer S, Pscherer A, Lichter P, Seiffert M. miRNA-130a targets ATG2B and DICER1 to inhibit autophagy and trigger killing of chronic lymphocytic leukemia cells. Cancer Res 2012; 7: 1763-72.

[34] Callegari E, Gramantieri L, Domenicali M, D'Abundo L, Sabbioni S, Negrini M. MicroRNAs in liver cancer: a model for investigating pathogenesis and novel therapeutic approaches. Cell Death Differ 2015; 1: 46-57.
[35] Weigel AL, Handa JT, Hjelmeland LM. Microarray analysis of H_2O_2-, HNE-, or tBH-treated ARPE-19 cells. Free Radic Biol Med 2002; 10: 1419-32.
[36] Halbeisen RE, Galgano A, Scherrer T, Gerber AP. Post-transcriptional gene regulation: from genome-wide studies to principles. Cell Mol Life Sci 2008; 5: 798-813.
[37] Farh KK, Grimson A, Jan C, Lewis BP, Johnston WK, Lim LP, Burge CB. The widespread impact of mammalian microRNAs on mRNA repress on and evolution. Science 2005; 16: 1817-21.
[38] Iorio MV, Croce CM. MicroRNA dysregulation in cancer: diagnostics, monitoring and therapeutics. A comprehensive review. EMBO Mol Med 2012; 3: 143-59.
[39] Cheng G. Circulating miRNAs: roles in cancer diagnosis, prognosis and therapy. Adv Drug Deliv Rev 2015; 3: 75-93.
[40] Murai M, Toyota M, Suzuki H, Satoh A, Sasaki Y, Akino K, Ueno M, Takahashi F, Kusano M, Mita H, Imai K. Aberrant methylation and silencing of the BNIP3 gene in colorectal and gastriccancer. Clin Cancer Res 2005; 3: 1021-27.
[41] Tan EY, Campo L, Han C, Turley H, Pezzella F, Gatter KC, Harris AL, Fox SB. BNIP3 as a progression marker in primary human breast cancer; opposing functions in in situ versus invasive cancer. Clin Cancer Res 2007; 13: 467-74.
[42] Giatromanolaki A, Koukourakis MI, Sowter HM, Sivridis E, Gibson S, Gatter KC, Harris AL. BNIP3 expression is linked with hypoxia-regulated protein expression and with poor prognosis in non-small cell lung cancer. Clin Cancer Res 2004; 16: 5566-71.
[43] Shaida N, Launchbury R, Boddy JL, Jones C, Campo L, Turley H, Kanga S. Expression of BNIP3 correlates with hypoxia-inducible factor (HIF)-1alpha, HIF-2alpha and the androgen receptor in prostate cancer and is regulated directly by hypoxia but not androgens in cell lines. Prostate 2008; 3: 336-43.
[44] Kubli DA, Ycaza JE, Gustafsson AB. Bnip3 mediates mitochondrial dysfunction and cell death through Bax and Bak. Biochem J 2007; 3: 407-415.
[45] Zhang Z, Yang X, Zhang S, Ma X, Kong J. BNIP3 upregulation and EndoG translocation in delayed neuronal death in stroke and in hypoxia. Stroke 2007; 5: 1606-13.
[46] Kanzawa T, Zhang L, Xiao L, Germano IM, Kondo Y, Kondo S. Arsenic trioxide induces autophagic cell death in malignant glioma cells by upregulation of mitochondrial cell death protein BNIP3. Oncogene 2005; 6: 980-91.
[47] Tracy K, Dibling BC, Spike BT, Knabb JR, Schumacker P, Macleod KF. BNIP3 is an RB/E2F target gene required for hypoxia-induced autophagy. Mol Cell Biol 2007; 17: 6229-42.
[48] Bellot G, Garcia-Medina R, Gounon P, Chiche J, Roux D, Pouysségur J, Mazure NM. Hypoxia-induced autophagy is mediated through hypoxia-inducible factor induction of BNIP3 and BNIP3L via their BH3 domains. Mol Cell Biol 2009; 10: 2570-81.
[49] Mazure NM, Pouysségur J. Atypical BH3-domains of BNIP3 and BNIP3L lead to autophagy in hypoxia. Autophagy 2009; 6: 868-79.
[50] Li Y, Wang Y, Kim E, Beemiller P, Wang CY, Swanson J, You M, Guan KL. Bnip3 mediates the hypoxia-induced inhibition on mammalian target of rapamycin by interacting with Rheb. J Biol Chem 2007; 49: 35803-13.
[51] Azad MB, Chen Y, Henson ES, Cizeau J, McMillan-Ward E, Israels SJ, Gibson SB. Hypoxia induces autophagic cell death in apoptosis-competent cells through a mechanism involving BNIP3. Autophagy 2008; 2: 195-204.
[52] Zhang H, Bosch-Marce M, Shimoda LA, Tan YS, Baek JH, Wesley JB, Gonzalez FJ, Semenza GL. Mitochondrial autophagy is an HIF-1-dependent adaptive metabolic response to hypoxia. J Biol Chem 2008; 16: 10892-903.
[53] Yang K, He M, Cai Z, Ni C, Deng J, Ta N, Xu J, Zheng J. A decrease in miR-150 regulates the malignancy of pancreatic cancer by targeting c-Myb and MUC4. Pancreas 2015; 3: 370-9.
[54] Mraz M, Chen L, Rassenti LZ, Ghia EM, Li H, Jepsen K, Smith EN, Kipps TJ. miR-150 influences B-cell receptor signaling in chronic lymphocytic leukemia by regulating expression of GAB1 and FOXP1. Blood 2014; 1: 84-95.
[55] Wu Q, Jin H, Yang Z, Luo G, Lu Y, Li K, Ren G, Fan D. miR-150 promotes gastric cancer proliferation by negatively regulating the pro-apoptotic gene EGR2. Biochem Biophys Res Commun 2010; 3: 340-5.
[56] Huang S, Chen Y, Wu W, Ou YN, Chen J, Li H, Liu X, Yao Y. miR-150 promotes human breast cancer growth and malignant behavior by targeting the pro-apoptotic purinergic P2X7 receptor. PLoS One 2013; 12: 807-17.
[57] Cao M, Hou D, Liang H, Hou D, Liang H, Chen X. miR-150 promotes the proliferation and migration of lung cancer cells by targeting SRC kinase signalling inhibitor 1. Eur J Cancer 2014; 5: 1013-24.
[58] Wang F, Ren X, Zhang X. Role of microRNA-150 in solid tumors. Oncol Lett 2015; 1: 11-16.
[59] Jiang X, Huang H, Li Z , Wang X, Gurbuxani S and Chen P. Blockade of miR-150 maturation by MLL-fusion/MYC/LIN-28 is required for MLL-

associated leukemia. Cancer Cell 2012; 4: 524-35.
[60] Watanabe A, Tagawa H, Yamashita J, Teshima K, Nara M, Iwamoto K, Kume M, Kameoka Y, Takahashi N, Nakagawa T. The role of microRNA-150 as a tumor suppressor in malignant lymphoma. Leukemia 2011; 8: 1324-34.